# Cage-Shaped Mo9 Chalcogenides: Promising Thermoelectric Materials with Significantly Low Thermal Conductivity

Tong Zhou, Bertrand Lenoir, Christophe Candolfi, Anne Dauscher, Philippe Gall, Patrick Gougeon, Michel Potel, Emmanuel Guilmeau

# Cage-shaped $Mo_9$ chalcogenides: promising thermoelectric materials with significant low thermal conductivity

Tong Zhou[1], Bertrand Lenoir[1], Candolfi Christophe[1] Anne Dauscher[1]

Philippe Gall[2,3], Patrick Gougeon[2], Michel Potel[2]

Emmanuel Guilmeau[4]

[1]Institut Jean Lamour, UMR 7198 CNRS-Nancy Université-UPVM, Ecole Nationale Supérieure des Mines de Nancy, Parc de Saurupt, 54042 Nancy, France

[2] Unité Sciences Chimiques de Rennes, Equipe Chimie du Solide et Matériaux UMR6226 CNRS Université de Rennes 1, Avenue de Général Leclerc, 35042 Rennes, France

[3]INSA de Rennes, 20 Avenue des Buttes de Coesmes, 35043Rennes, France

[4]Laboratorie CRISMAT, CNRS-ENSICAEN, 6 Bld Marechal Juin, 14050 Caen, France

**Abstract**

Thermoelectric properties of molybdenum selenides containing $Mo_9$ clusters have been investigated between 300-800 K. $Ag_xMo_9Se_{11}$ ($x$ = 3.4 and 3.8) have been synthesized by solid state reactions and spark plasma sintering. X-ray diffraction and scanning electron microscope reveal high purity and good homogeneity of the samples. The thermoelectric power of the samples is positive in the whole temperature, indicating that the majority of charge carriers are holes. The Seebeck coefficient increases with temperature, and the temperature coefficient of the resistivity is positive. Significant low thermal conductivity, comparable to those values reported in the state-of-

the-art thermoelectric materials, is observed in this new system, and this is assumed to be associated with rattling effect from the Ag filler atoms. It has been demonstrated that the electrical and thermal properties correlate to the Ag concentration. For $x = 3.8$, a promising dimensionless thermoelectric figure of merit of ~ 0.7 is obtained at 800K.

## Introduction

The challenge in any effort to discover new thermoelectric materials lies in achieving simultaneously high thermoelectric power *S*, low electrical resistivity ρ and low thermal conductivity λ.[1, 2] These properties define the dimensionless figure of merit $ZT = (S^2/\rho\lambda)T$, which indicates the efficiency of thermoelectric materials. The total thermal conductivity λ is given as the sum of the lattice ($\lambda_l$) and electronic ($\lambda_e$) contributions. The latter part is correlated to the electronic structure based on the Wiedemann-Franz law. *S*, ρ and $\lambda_e$ are determined by the details of the electronic structure and scattering of charge carriers (electrons or holes) and therefore are not independently controllable. An effective way to maximize the ZT value is to manipulate the lattice thermal conductivity $\lambda_l$, which is the only parameter not determined by the electronic structure. One of the strategies to reduce $\lambda_l$ is to look at compounds possessing open cages which can be filled with rattlers. Phonons can be scattered more strongly than electrons (or holes) in such a crystal structure, and the lattice thermal conductivity is reduced as a result.[3, 4] This concept has been successfully demonstrated in several classes of materials, such as filled-Skutterudites,[2, 5] $Zn_4Sb_3$-based materials,[6] Clathrates[7] and semiconducting Chevrel phases.[8-10]

Most of Chevrel compounds can be described by the formula $MMo_6X_8$, where M = alkaline, alkaline earth, transition metal, rare earth or actinide and X is usually a chalcogen (S, Se, Te).[11] The fundamental structural unit $Mo_6X_8$ is the octahedral cluster $Mo_6$ surrounded by eight chalcogens in a distorted cube. $Mo_6X_8$ units build up a progression of channels where accommodate a variety of atoms. Some of these filler atoms, e.g. Cu, Fe and Ni, show large thermal motions, indicating that they undergo rattling inside their oversized cages and can effectively scatter the phonons.[12] The thermal conductivity in the unfilled Chevrel phase $Mo_6Se_8$ is about 7 W/mK at room temperature.[8] This value can be significantly lowered by filling up atoms in the voids. Up to

date, the lowest thermal conductivity of ~ 1.3W/mK (300 K) has been reported in the Cu filled $Mo_6Se_8$ where Cu has a thermal parameter about two order of magnitude larger compared to those for large filler atoms such as La or Sn and also those for Mo and Se atoms in the framework.[8] The best ZT value of 0.6 (1150K) is reported in the Cu/Fe filled composition.[8] However, there should be some concern that the ionic mobility of small filler atoms may lead to degradation of the material under operating conditions.[13]

Our study focuses on evaluating the thermoelectric potential of other ternary molybdenum selenides with higher nuclearity Mo clusters (bioctahedral $Mo_9$).[14-16] The crystal structure is built up by interconnected $Mo_9Se_{11}$ units, which can be described as the results of the uniaxial face-sharing condensation of two $Mo_6Se_8$ units with loss of Se atoms belonging to the shared face. The metal-metal and metal-chalcogen distances in this larger cluster are in the same range as in the $Mo_6X_8$ clusters, but Mo-Mo bonds between $Mo_3X_3$ layers are slightly longer than within layers. The metal atoms in the top and bottom layers are very similar in their environment to the metal atoms in $Mo_6X_8$. The building blocks of $Mo_9Se_{11}$ form a framework with voids where a variety of atoms may reside. Similar to the Chevrel phase, there is considerable variability in positioning and stoichiometry with regard to the filler atoms. In addition, other transition metals can be substituted for Mo. These fillings and substitutions can be used to monitor the electronic behaviour of these compounds. This is beneficial from a thermoelectric standpoint. Of importance, similar to Chevrel phases, the $Mo_9$ compounds have also complicated structures with high degree of disorder, which may lead to low lattice thermal conductivity. In this paper we present for the first time a systematic study of thermoelectric properties on polycrystallines Ag filled $Mo_9Se_{11}$ ($Ag_{\sim 3.6}Mo_9Se_{11}$ orthorhombic phase) in the 300-800K temperature range. The obtained values have been compared to those reported in the Cu/Fe filled Chevrel compound.[8]

**Experimental Section**

High purity starting materials (Ag, Mo powders and Ag shots) were used for the solid state reaction.[14, 17] Mo powder was reduced under $H_2$ flowing gas at high temperature in order to eliminate any trace of oxygen. In the first step, molybdenum diselenide was prepared by a direct reaction of selenium with molybdenum in a sealed silica tube. $Ag_xMo_9Se_{11}$ ($3.4<x<3.8$) samples were obtained by heating the required stoichiometric mixture of Ag, Mo and $MoSe_2$ in a sealed tube at 1000-1100$^o$C for one day. The synthesized powders were densified by Spark Plasma Sintering (SPS) at between 1000-1100$^o$C for 10 minutes at 80MPa resulting in dense samples (> 91 % of the theoretical density). In our study, small variations in the Ag concentration (nominal 3.4 and 3.8 respectively) were made to examine the effect of stoichiometry on the physical properties.

The X-rays diffraction was examined on a Bruker D8 diffractometer equipped with a germanium monochromator (only $CuK_{\alpha 1}$ employed) and a LynxEye detector. The information on the lattice unit cell was obtained via the Rietveld refinement. The thermopower and the electrical resistivity were measured simultaneously by a ULVAC-ZEM3 device under partial helium atmosphere. The heat capacity and the thermal diffusivity measurements were carried out on Netzsch DSC 404C and LFA-457 models respectively. The density at 300 K was evaluated by measuring the volume and the mass of the samples. The thermal conductivity was estimated using the product of the density, the thermal diffusivity and the heat capacity assuming that the density is temperature independent. All the thermal and electrical properties were measured between 300-800K. Uncertainties in the electrical resistivity and thermal conductivity are ± (2-7)% due in large part in determination of the sample dimensions; the uncertainties in the thermopower are ± 4%. Thus the uncertainty in the ZT is around 17%.

**Results and Discussions**

Figure 1 presents the projections of the $Ag_xMo_9Se_{11}$ structure onto (001) and (100) planes from the data of Gougeon et al.[14] There are four Ag sites crystallographically independent. The silver non-stoichiometry arises essentially from the filling of the Ag4 site located in rhomboid cross-section channels extending along the *a* direction, as seen in Figure 1b. It is worthy to pay attention to very large thermal motion on this Ag4 site, which is clearly demonstrated regarding the size of the ellipsoids. This situation may produce a phonon damping effect that results in a dramatic decrease of the phonon mean free path and hence a reduction of the lattice thermal conductivity.

The XRD patterns in Figure 2 reveal that the main phase in both samples can be indexed to $Ag_xMo_9Se_{11}$.[14] As seen in the inset of Figure 2, the SEM image presents a dense and quite homogeneous microstructure of a sintered sample. The $Ag_{3.8}Mo_9Se_{11}$ has bigger unit cell size (*a* = 11.9103(2)Å, *b* = 13.6304(2)Å and *c* = 11.6801(2)Å V=1896.2(1) $Å^3$)) compared to $Ag_{3.4}Mo_9Se_{11}$ (*a* = 11.9013(3)Å, *b* = 13.5934(3)Å and *c* = 11.6694(3)Å V=1887.9(1)$Å^3$)). The cell volume usually increases as the concentration of filler atoms increases. Even though the in-house XRD does not provide good statistics on precise Ag occupancy, the refined lattice parameters of each sample can be a good indicator of different Ag filling levels. This can also be confirmed by referring to the previously reported lattice parameters of single crystal $Ag_{3.60}Mo_9Se_{11}$ $Ag_{3.60}Mo_9Se_{11}$ (*a* = 11.910(3) Å, *b* = 13.614(4) Å and *c* = 11.679(3)Å) and $Ag_{3.76}Mo_9Se_{11}$ (*a* = 11.926 Å, *b* = 13.619Å and *c* = 11.661(9)Å).[14, 17]

The electrical resistivity as a function of temperature is displayed in Figure 3 for the two samples investigated. Also shown in this figure is the result for $(Cu/Fe)Mo_6Se_8$ according to Caillat *et al.*[8] For $Ag_xMo_9Se_{11}$ samples the ρ increases with temperature in the temperature range measured, indicating of a metallic behaviour. A similar behaviour is encountered in the Chevrel compound but with lower resistivity values. With respect to the Chevrel phases, one of the most

important electronic parameters is the metallic electron count (MEC), i.e. the number of electrons that are available for metal-metal bonding. It can be calculated by adding the oxidation number of filler atoms(s) to the valence electrons of the cluster atoms ($Mo_6$:36, $Mo_9$:54) by subtracting the number of electrons necessary to complete the octets of the chalcogen atoms. The MEC is a convenient measure for the degree of filling of the conduction band, which lies near the Fermi level.[11] Based on band structure calculations, Chevrel phases are formed for MEC between 20 and 24. A value of 24 can be obtained by either substitution on metal sites or filling the voids. Mixed clusters such as $Mo_4Ru_2Se_8$ or $Mo_2Re_4Se_8$ and the Ti filled $Mo_6Se_8$ are found to be semiconductors.[8, 18, 19] The compositions with a MEC lower than 24 are generally metallic and this has been also experimentally confirmed in the Chevrel compounds inserted with Cu, Cu/Fe or Ag atoms.[8, 20] For the $Mo_9$ cluster, a previous theoretical study has shown that the MEC varies from 32 to 36.[16] A MEC of 35.6 has been characterized in $Ag_{3.6}Mo_9Se_{11}$.[14] In our results, $Ag_{3.8}Mo_9Se_{11}$ has higher resistivity than $Ag_{3.4}Mo_9Se_{11}$, and this corresponds to their different MEC which govern Mo-Mo intercluster distances and hence determine electronic properties.

Figure 4 shows the temperature dependance of the thermopower for the $Ag_xMo_9Se_{11}$ samples in comparison with that of (Cu/Fe)$Mo_6Se_8$.[8] As for the latter compound, our samples present positive thermoelectric power over the whole temperature range investigated, suggesting that holes dominate the electrical transport. The *S* increases with temperature for both $Ag_xMo_9Se_{11}$ samples, consistent with the systematic change of the resistivity. In addition, the *S* increases as the Ag concentration increases, ranging from ~ 140 μV/K for $x$ = 3.4 to ~ 175 μV/K for $x$ = 3.8 at 800K, values that are higher than that reported in (Cu/Fe)$Mo_6Se_8$.

The very promising aspect of our preliminary study is the magnitude of the thermal conductivity of the ternary $Ag_xMo_9Se_{11}$ compounds. As seen in Figure 5, the thermal conductivity for both samples is slightly temperature dependent, and is lower than that of the (Cu/Fe)$Mo_6Se_8$

which has the lowest λ record in the Chevrel family. Such low thermal conductivity displayed by these $Mo_9$ clusters selenides could be attributed to the complex crystalline structure, where interplay between static and dynamic disorder could exist. The thermal parameter was used to probe the disorder in the cage-like structures, where rattling effect has been observed. [12] The ambient temperature thermal parameter of a rattler atom can be at least three to ten times larger than that of the other atom types in the structure with comparable masses.[12] Take an example of the single crystal structure interpretation of $Ag_{3.6}Mo_9Se_{11}$: the equivalent isotropic room temperature thermal parameter of Ag, $U_{iso}$(Ag), is 3.45Å$^2$, much higher than that of Mo (0.48 Å$^2$) and Se (0.81 Å$^2$). Interestingly, the λ has been found linked to the Ag concentration, and it decreases by nearly 30% as $x$ increases from 3.4 to 3.8. Presumably, higher Ag concentrations create higher degree of disorder with a random mixture of filling Ag and vacancies inside the voids. In this way, the phonon scattering is strongly enhanced. Therefore, one can conclude that the Ag concentration has influence not only on the electronic properties but also on lattice vibrations of phonons.

The power factor (PF) and the dimensionless ZT are evaluated based on the above discussed transport data, as shown in Figure 6. Both samples show similar temperature dependence of PF, which reaches ~ 630 μW/mK$^2$ at 800K. Higher ZT values observed in $Ag_{3.8}Mo_9Se_{11}$ is attributed to its lower thermal conductivity compared to that of $Ag_{3.4}Mo_9Se_{11}$. A ZT value of ~ 0.7 is obtained at 800K for $x$ = 3.8. This is more than twice the value reported in (Cu/Fe)$Mo_6Se_8$ which is the best compound.[8]

**Conclusion**

We explore for the first time the thermoelectric properties of the $Mo_9$ clusters selenides partially filled with Ag atoms, namely $Ag_xMo_9Se_{11}$. We show that it is possible to tune the electric

properties by varying the Ag concentration. The thermal conductivity of these compounds is surprisingly low and this might be attributed to the Ag rattling effect. The largest ZT value measured so far is ~ 0.7 at 800K for $Ag_{3.8}Mo_9Se_{11}$. The dependence of the thermoelectric properties on the filling concentration suggests that there is further room for ZT improvement. These encouraging results suggest the family of $Mo_9$ selenides a new category of possible thermoelectric materials for investigation.

## Figure Captions

Figure 1 The perspective view of the $Ag_xMo_9Se_{11}$ structure (space group: *Cmcm*) (a) along the *c* axis and (b) the *a* axis. The ellipsoids of Ag atoms demonstrate their thermal motion in the oversized cages.

Figure 2 XRD patterns for $Ag_{3.4}Mo_9Se_{11}$ (bottom) and $Ag_{3.8}Mo_9Se_{11}$ (top). Inset: the SEM image of the sample of $Ag_{3.8}Mo_9Se_{11}$.

Figure 3 Temperature dependence of resistivity for $Ag_{3.4}Mo_9Se_{11}$ (square) and $Ag_{3.8}Mo_9Se_{11}$ (triangular), in comparison with $(Cu/Fe)Mo_6Se_8$ (cross).

Figure 4 Temperature dependence of the thermopower for $Ag_{3.4}Mo_9Se_{11}$ (square) and $Ag_{3.8}Mo_9Se_{11}$ (triangular), in comparison with $(Cu/Fe)Mo_6Se_8$ (cross).

Figure 5 Temperature dependence of the thermal conductivity for $Ag_{3.4}Mo_9Se_{11}$ (square) and $Ag_{3.8}Mo_9Se_{11}$ (triangular), in comparison with $(Cu/Fe)Mo_6Se_8$ (cross). All the data for $Ag_xMo_9Se_{11}$ samples have been corrected to take into account the relative density of the different samples. [21]

Figure 6 Temperature dependence of the dimensionless ZT value for $Ag_{3.4}Mo_9Se_{11}$ (square) and $Ag_{3.8}Mo_9Se_{11}$ (triangular), in comparison with $(Cu/Fe)Mo_6Se_8$ (cross).

## References


[1] D. M. Rowe, *CRC Handbook of Thermoelectrics* (CRC, Boca Raton, 1995).

[2] D. M. Rowe, *CRC Handbook of Thermoelectrics: macro to nano* (CRC, Boca Raton, 2005).

[3] J. R. Sootsman, D. Y. Chung, and M. G. Kanatzidis, ANGEW CHEM INT EDIT **48**, 8616 (2009).

[4] G. J. Snyder, and E. S. Toberer, NAT MATER **7**, 105 (2008).

[5] B. C. Sales, D. Mandrus, and R. K. Williams, Science **272**, 1325 (1996).

[6] H. J. Kim, E. S. Božin, S. M. Haile, G. J. Snyder, and S. J. L. Billinge, PHYS REV B **75**, 134103 (2007).

[7] G. S. Nolas, J. L. Cohn, G. A. Slack, and S. B. Schujman, APPL PHYS LETT **73**, 178 (1998).

[8] T. Caillat, J. P. Fleurial, and G. J. Snyder, SOLID STATE SCI **1**, 535 (1999).

[9] R. W. Nunes, I. I. Mazin, and D. J. Singh, PHYS REV B **59**, 7969 (1999).

[10] C. Roche, R. Chevrel, A. Jenny, P. Pecheur, H. Scherrer, and S. Scherrer, PHYS REV B **60**, 16442 (1999).

[11] E. Kaldis, *Current Topics in Materials Science* (North-Holland, Amsterdam, 1979), Vol. 3.

[12] B. C. Sales, B. C. Chakoumakos, D. Mandrus, and J. W. Sharp, J SOLID STATE CHEM **146**, 528 (1999).

[13] E. Levi, G. Gershinsky, D. Aurbach, O. Isnard, and G. Ceder, CHEM MATER **21**, 1390 (2009).

[14] P. Gougeon, J. Padiou, J. Y. L. Marouille, M. Potel, and M. Sergent, J SOLID STATE CHEM **51**, 218 (1984).

[15] P. Gougeon, M. Potel, and R. Gautier, INORG CHEM **43**, 1257 (2004).

[16] S. Picard, J.-F. Halet, P. Gougeon, and M. Potel, INORG CHEM **38**, 4422 (1999).

[17] P. Gougeon, M. Potel, J. Padiou, and M. Sergent, CR ACAD SCI **297**, 351 (1983).

[18] T. Caillat, and J.-P. Fleurial, J SOLID STATE CHEM **59**, 1139 (1998).

[19] M. A. McGuire, A. M. Schmidt, F. Gascoin, G. Jeffrey Snyder, and F. J. DiSalvo, J SOLID STATE CHEM **179**, 2158 (2006).

[20] X.-y. Shi, L. Wang, L.-d. Chen, and X.-h. Chen, T NONFERR METAL SOC **19**, 642 (2009).

[21] R. Landauer, J APPL PHYS **23**, 779 (1952).

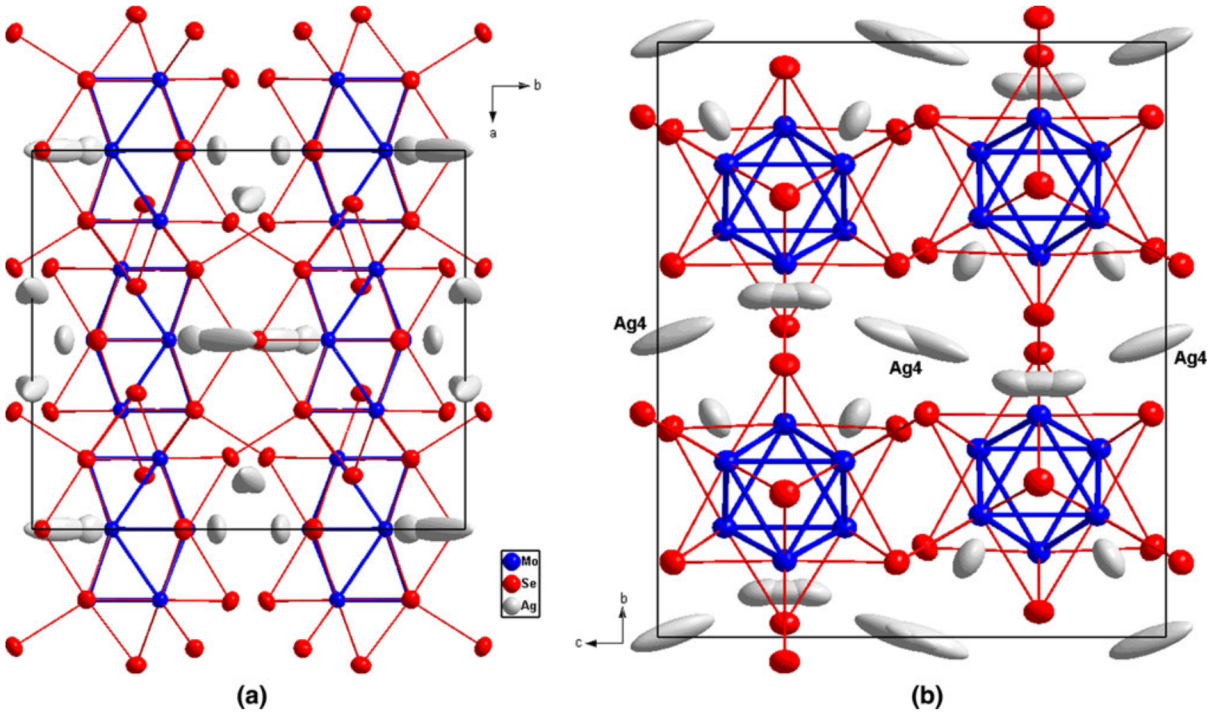


Figure 1

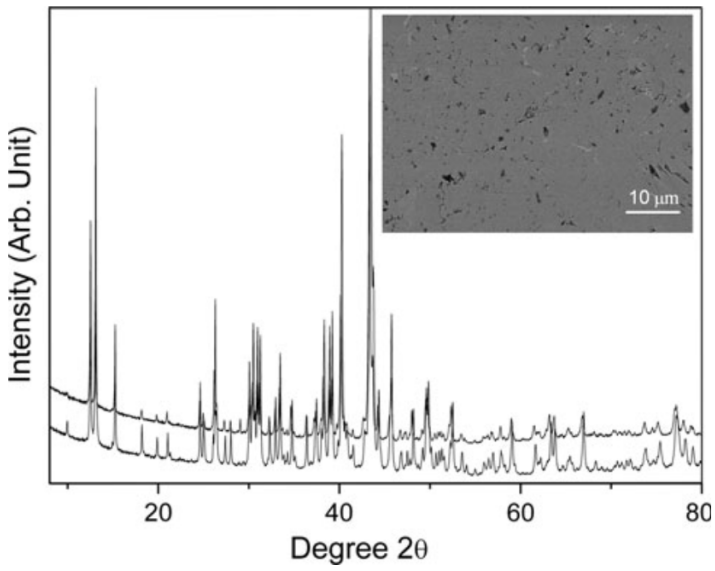


Figure 2

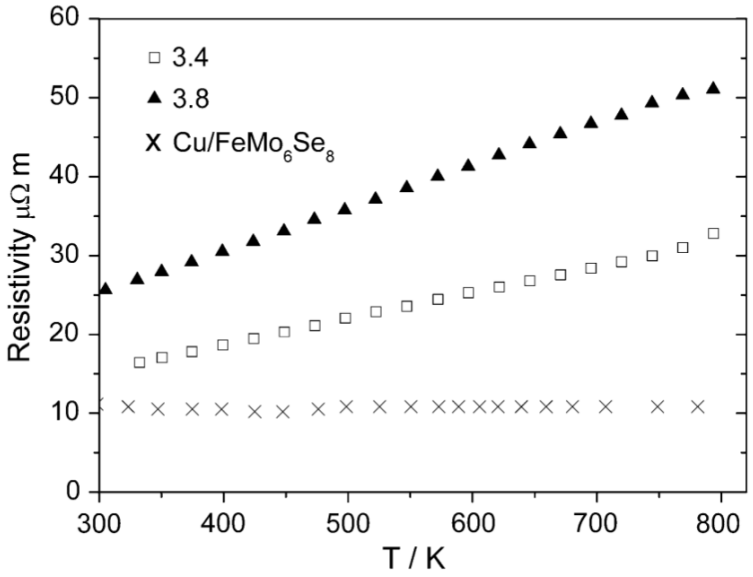
60
50
40
30
20
10
0
Resistivity μΩ m
3.4
3.8
X Cu/FeMo6Se8
300
400
500
600
700
800
T / K

Figure 3

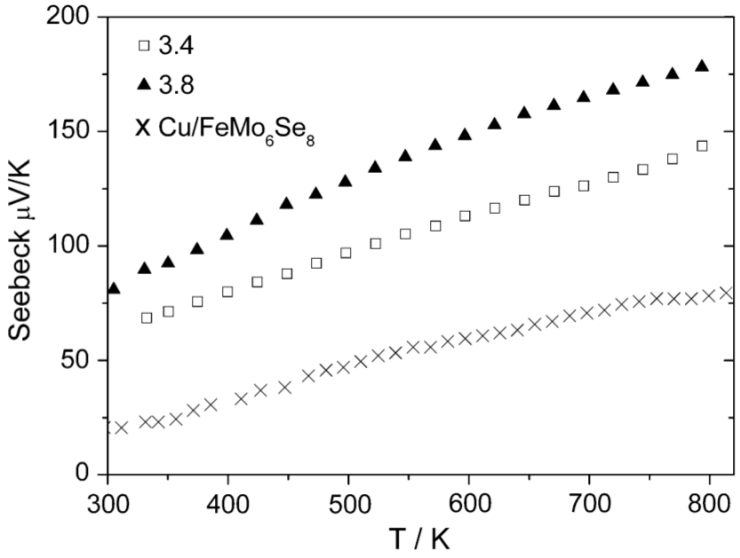
200
150
100
50
0
Seebeck μV/K
3.4
3.8
X Cu/FeMo6Se8
300
400
500
600
700
800
T / K

Figure 4

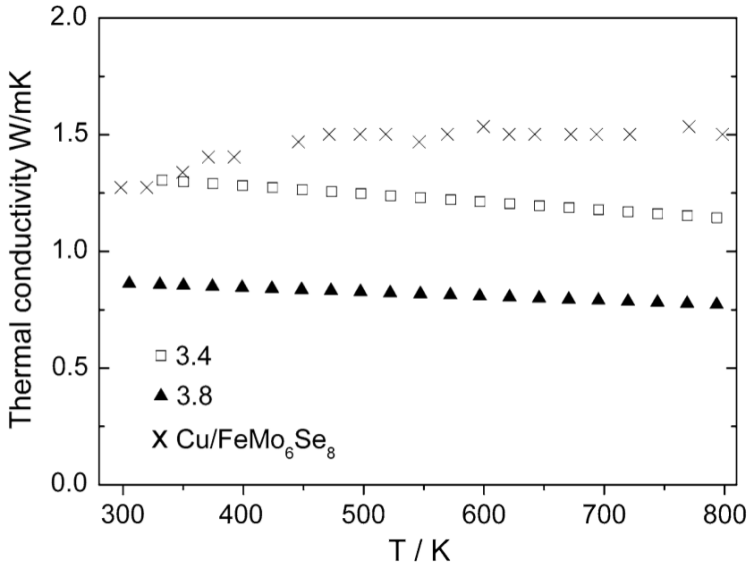
Thermal conductivity W/mK
2.0
1.5
1.0
0.5
0.0
300
400
500
600
700
800
T / K
3.4
3.8
Cu/FeMo6Se8

Figure 5

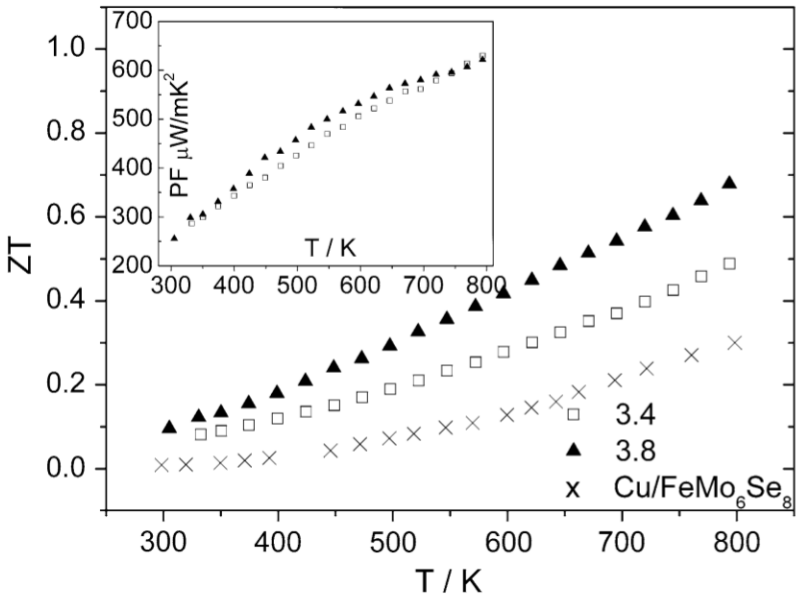


Figure 6